http://dx.doi.org/10.5935/0103-5053.20150019

*J. Braz. Chem. Soc.*, Vol. 26, No. 4, 633-641, 2015.
Printed in Brazil - ©2015 Sociedade Brasileira de Química
0103 - 5053 $6.00+0.00

Article

# Novel *N*-Acylated Benzimidazolone Derivatives: Synthesis, 2D-QSAR and Targets Prediction

***Shaopeng Wei and Zhiqin Ji****

*College of Plant Protection and State Key Laboratory of Crop Stress Biology in Arid Areas, Northwest A&F University, Yangling, 712100 Shaanxi, P. R.China*

A series of novel *N*-acylated benzimidazolone derivatives, were synthesized from 4-aminobenzoic acid, and their antifungal activities against *Botrytis cinerea* were evaluated by spore germination assay. Preliminary results indicated that most of the benzimidazolone derivatives had inhibitory effect on spore germination, among which 6-carboxylate substituted derivatives were more effective than its 5-substituted regioisomers. Furthermore, 2D-quantitative structure-activity relationship (2D-QSAR) studies revealed good predictive and statistically significant QSAR models, as well as highlighted that the activities were strongly influenced by the type of introduced acyl groups in the benzimidazolone moiety. Potential targets of the title compounds were predicted using ligand profiling and validated by molecular docking, and the results implied that the title compounds might be a new type of fatty acid synthetase inhibitor.

**Keywords:** benzimidazolone, antifungal activity, 2D-QSAR, targets prediction

## Introduction

Benzimidazolone derivatives are widely distributed in a variety of pharmacological compounds, such as antagonists of non-nucleoside HIV-1 RT (NNRTIs),[1] calcitonin gene-related peptide (CGRP),[2] p53-Mdm2,[3] cannabinoid receptor 2 (hCB2),[4] opioid receptor-like 1 (NOP),[5,6] *N*-methyl-daspartate (NMDA)[7] and mGlu5 receptors,[8] as well as inhibitors of *Mycobacterium tuberculosis* enzyme,[9] non-nucleoside reverse transcriptase,[1] *D*-amino acid oxidase (DAAO)[7] and heat shock protein 90 (HSP90).[10] Benzimidazolone carboxylic acids derivatives are potential therapeutic agents of selective peroxisome proliferator-activated receptor γ modulators (SPPARγMs), and may be used to treat type II diabetes mellitus (T2DM).[11] However, literature survey shows that there were only a few reports on the antimicrobial activity of benzimidazolones. Benzimidazolone derivatives bearing a sugar residue or piperidine ring on the aromatic nitrogen were synthesized and found to have strong antibacterial activity.[12,13] In our previous investigation, a series of *N*-acylated benzimidazolone derivatives were synthesized by introducing acyl groups to the nitrogen atom of 1-isopropenylbenzimidazolone, and were subjected to evaluate their antifungal activity against *Botrytis cinerea*.[14-16] As a continuation of this work, especially to investigate the effects of substituted groups at aromatic moiety on the activity, the pharmaceutical profile was optimized by introducing ethyl carboxylate at 5- and 6-positions. Two dimensional-quantitative structure-activity relationship (2D-QSAR) studies were performed to correlate between the structures and antifungal activities of the title compounds. Moreover, potential targets of the title compounds were predicted using ligand profiling methods from PharmaDB pharmacophore database (sc-PDB) and validated by molecular docking based on Discovery Studio software.

*e-mail: jizhiqin@nwsuaf.edu.cn

## Methodology

### General methods

Melting points were measured on a WPR apparatus and uncorrected (Shanghai Jingke Co., China). $^{1}$H nuclear magnetic resonance (NMR) and $^{13}$C NMR spectra were recorded on a Bruker AVANCE III NMR spectrometer (Bruker Daltonics Inc., Germany), using tetramethylsilane ($Me_4Si$) as an internal standard ($^{1}$H at 500 MHz, $^{13}$C at 125 MHz, respectively). Elemental analyses were carried out on an Elementar Vairo EL analyzer (Elementar Analysensysteme Co., Germany). Reaction progress was monitored by thin-layer chromatography (TLC) on

silica gel GF254 with visualization by ultraviolet. Silica gel (200-300 mesh; Qingdao Chemical Co., China) was used for column chromatography mixtures of petroleum ether and ethyl acetate. The purities of tested compounds were determined to be greater than 95% based on reverse-phase high-performance liquid chromatography (HPLC) analysis.

### Synthesis of compounds **11a01-11a15**

To a stirred solution of ethyl 4-amino-3-nitrobenzoate **5** (2.10 g, 10 mmol) in 25 mL dichloromethane (DCM) were added 3.0 mL triethylamine ($Et_3N$). Isobutyl chloroformate (2.04 g, 15 mmol) in 10 mL DCM was added dropwise in an ice-water bath and the mixture was stirred for 5 h at room temperature. To the reaction solution was added 50 mL of saturated $NaHCO_3$ aqueous solution, and the mixture was stirred for 30 min at room temperature. After this time, the aqueous layer was extracted with DCM (3 × 20 mL), and the organic extracts were combined, washed with water and brine, dried over $Na_2SO_4$, and concentrated under reduced pressure. The residue was purified by silica gel column chromatography eluted with petroleum ether and ethyl acetate (5/1, v/v) to give compound **6a** (2.01 g, 64.8% yield) as a yellow solid; m.p.: 85.5-87.3 °C.

To compound **6a** (1.55 g, 5 mmol) were added 20 mL ethanol and 40 mL water at room temperature. The mixture was heated to reflux, and then the solution of $Na_2S_2O_4$ (2.61 g, 15 mmol) in 40 mL water was added dropwise. After stirring for 0.5 h, the mixture was cooled to room temperature, and extracted with ethyl acetate (3 × 50 mL). The combined organic layers were washed with brine, dried over $Na_2SO_4$, and concentrated under reduced pressure to afford compound **7a** (1.33 g, 95.0% yield) as a yellow solid; m.p.: 108.3-109.4 °C.

To a stirred solution of compound **7a** (1.40 g, 5 mmol) in 15 mL of anhydrous tetrahydrofuran (THF) was added *N*,*N*-carbonyl-diimidazole (CDI, 1.62 g, 10 mmol). The reaction mixture was stirred for 20 h at room temperature. The solvent was removed under reduced pressure. The residue was diluted with 10 mL of water, extracted with ethyl acetate (3 × 50 mL). The combined organic layers were washed with brine, dried over $Na_2SO_4$, filtered and concentrated to give a brown solid. Purification by silica gel column chromatography eluted with petroleum ether and ethyl acetate (3/1, v/v) to give compound **8a** (1.31 g, 85.6% yield) as a white solid; m.p.: 164.6-166.0 °C.

To a stirred solution of **8a** (1.53 g, 5 mmol) in 20 mL of dimethylformamide (DMF) was added $K_2CO_3$ (2.07 g, 15 mmol) and 2-iodopropane (1.02 g, 6 mmol). The mixture was stirred at room temperature for 24 h. TLC analysis showed the reaction completion. The mixture was diluted with 50 mL of water and extracted with ethyl acetate (3 × 50mL). The combined organic layers were washed with brine, dried over $Na_2SO_4$, and concentrated under reduced pressure to afford a brown solid. Purification by silica gel column chromatography eluted with petroleum ether and ethyl acetate (4/1, v/v) gave compound **9a** (1.37 g, 78.7% yield) as a white solid; m.p.: 88.2-89.8 °C.

To a stirred solution of **9a** (1.74 g, 5 mmol) in 20 mL of DCM were added 0.5 mL trifluoroacetic acid (TFA). The mixture was stirred at room temperature for 24 h. TLC analysis showed the reaction completion. The mixture was diluted with 50 mL of water and extracted with ethyl acetate. The combined organic layers were washed with brine, dried over $Na_2SO_4$, and concentrated under reduced pressure to afford a brown solid. Purification by silica gel column chromatography eluted with petroleum ether and ethyl acetate (2/1, v/v) gave compound **10a** (1.05 g, 85% yield) as a white solid; m.p.: 175-176 °C.

The title compounds **11a01-11a15** were prepared by acylation of **10a** with the corresponding acyl chlorides. Their structures were characterized by $^1$H NMR, $^{13}$C NMR and elemental analysis.

### Synthesis of compounds **9b01-9b21**

To a stirred solution of **5** (2.10 g, 10 mmol) in 50 mL of anhydrous THF was added acetone (1.2 mL, 16 mol), *p*-toluenesulfonic acid (PTSA, 3.00 g, 17 mmol) and $NaBH_4$ (0.50 g, 15 mmol). The mixture was stirred at room temperature for 2 h. TLC analysis showed the reaction completion. The mixture was neutralized with saturated $NaHCO_3$ aqueous solution and extracted with DCM (3 × 50 mL). The combined organic layers were washed with brine, dried over $Na_2SO_4$, and concentrated under reduced pressure to afford a brown solid. Purification by silica gel column chromatography eluted with petroleum ether and ethyl acetate (1/1, v/v) gave compound **6b** (2.17 g, 86% yield) as a yellow solid; m.p.: 127-129 °C.

The nitro group of **6b** was reduced as described for **6a** to afford compound **7b** (92% yield) as a thick liquid.

To a stirred solution of compound **7b** (1.11 g, 5 mmol) in 15 mL anhydrous DCM was added triphosgene (2.5 mL, 20% in DCM) dropwise. The reaction mixture was stirred for 16 h at room temperature; the reaction was quenched with saturated $NaHCO_3$ aqueous solution, and the mixture was extracted with DCM (3 × 50 mL). The combined organic layers were washed with brine, dried over $Na_2SO_4$, filtered and concentrated under reduced pressure to give a brown solid. Purification by silica gel column chromatography eluted with petroleum ether and

ethyl acetate (2/1, v/v) gave compound **8b** (0.94 g, 76% yield) as a white solid; m.p.: 171-172 °C.

The title compounds **9b01**-**9b21** were prepared by acylation of **8b** with the corresponding acyl chlorides. Their structures were characterized by $^{1}$H NMR, $^{13}$C NMR and elemental analysis.

### Antifungal activity

The tested fungal pathogen, *Botrytis cinerea* (PPC-B01), was provided by the Institute of Plant Disease, Northwest A&F University. The strain was retrieved from the storage tube and cultured for 2 weeks at 20 °C on potato dextrose agar (PDA, Difco, USA). Plates were then flooded with sterile distilled water, and conidia were scraped with a glass stick. Mycelial debris was removed by filtration through double-layer cheesecloth, and the spores were harvested and suspended in sterile distilled water containing 0.1% (v/v) Tween 20. Spores were counted using a hemocytometer and adjusted to $1.0 \times 10^6$ spores mL$^{-1}$.

The inhibitory effect of the title compounds against the spore germination of *B. cinerea* was determined using a method previously reported.[14] The tested samples (10 mg) dissolved in dimethyl sulfoxide (DMSO, 1 mL) were diluted 100 times with sterile distilled water to afford tested solution (100 μg mL$^{-1}$). The samples were inoculated with equal volume of spore suspension of *B. cinerea* containing $1.0 \times 10^6$ spores mL$^{-1}$. Aliquots of 10 μL of prepared spore suspension were placed on separate glass slides in triplicate. Slides containing the spores were incubated in a moisture chamber at 25 °C for 6 h. Each slide was then observed under the microscope for spore germination. The spore-generated germ tubes were enumerated, and percentage of spore germination was calculated.

### Effects of exogenous fatty acid on the antifungal activity of benzimidazolones

Except for adding equal amounts of sodium stearate to the tested solution, the other steps were performed according to the procedure above.

### QSAR studies

The chemical structures of all compounds were built initially using Chemoffice 2006 and subsequently exported to Accelrys Discovery Studio 4.0.[17] All geometries were optimized by Merck Molecular Force Field (MMFF) force fields, and then their energies were minimized using the steepest descent followed by conjugate gradient algorithms with a convergence gradient value of 0.01 kcal mol$^{-1}$. Optimization methods were used followed by conformational search of each energy-minimized structure.

The most stable conformer of each structure was selected and saved into the database to generate the common descriptors. Thirty-six *N*-acylated benzimidazolone carboxylates with antifungal activities were selected for QSAR analyses, and various physicochemical properties were selected as descriptors for initial QSAR construction, including 2D (AlogP, molecular weight, number of hydrogen acceptors, number of hydrogen donors, number of rotatable bonds, topological descriptors, etc.) and 3D (dipole, Jurs descriptors, shadow indices, molecular volume, molecular surface area, etc.) parameters.

To develop the QSAR model, the antifungal activity data were expressed as inhibition percentage and transferred as *D* values according equation 1, and the statistical techniques were used with genetic function algorithm (GFA) and partial least squares (PLS) in Discovery Studio. GFA algorithm is a new approach for building the QSAR models. Replacing regression analysis with the GFA algorithm allows the construction of models competitive with or superior to those produced by standard techniques and makes available additional information not provided by other techniques. Unlike most other analysis algorithms, GFA enables multiple models where the populations of the models are created by evolving random initial models using a genetic algorithm. GFA cannot only build linear models but also higher-order polynomials, splines, and other nonlinear functions.[18]

$$D = \lg [a / (100 - a)] + \lg M \quad (1)$$

where *a* is inhibition percentage and M is molecular weight of the compound. With compound **11a01** as reference, *a* is 46.65, M = 290.314, then *D* value was calculated as 2.40 according to equation 1.

### Target prediction and molecular docking

Ligand profiling is an emerging computational method for predicting the most likely targets of a bioactive compound and therefore anticipating adverse reactions, side effects and drug repurposing.[19] In this study, potential targets of the title compounds were predicted using the ligands profiler protocol from the built-in sc-PDB database based on the software Accelrys Discovery Studio 4.0. The sc-PDB database (release 2010) is the largest ever reported collection of structure-based pharmacophores derived from 7,687 protein-ligand X-ray structures. A total of 7,687 sc-PDB complexes yielded at least one valid pharmacophore. Altogether, the PharmaDB collection totals 139,482 pharmacophores from 3,034 different targets and 5,339 unique ligands.[20]

The conformer database of the title compounds was generated using the default fast setting of the conformation generation component and mapped to no-shape PharmaDB pharmacophores using the default setting of the ligand profiler protocol in Discovery Studio (DS). For each compound, targets were ranked by decreasing fit values. The pharmacophores that mapped well with active compounds were further screened by analyzing the source of the related protein. The crystal structure of the potential protein was downloaded from the Research Collaboratory for Structural Bioinformatics (RCSB) Protein Data Bank and utilized in molecular docking.[21]

Molecular docking calculations were performed using CDOCKER protocol available in DS. Prior to docking, the co-crystallized with inhibitor was prepared using prepare protein protocol in DS, during which the protein was typed with CHARMm force field, hydrogen atoms were added, water molecules were deleted and protonation states were assigned. The active site was defined as a sphere that comes within 10.0 Å from the geometric centroid of the inhibitor molecule (x = 49.271, y = 52.144, z = 36.982). Default setting for small molecule-protein docking was used throughout the simulation.

In order to validate CDOCKER as a suitable docking program for the binding mode prediction, the origin docking was performed. Original ligand was docked in the defined active site and ten best docking poses were inspected visually and compared to the binding mode in the crystal structure of the complex. We evaluated various scoring (CDOCKER_ENERGY, CDOCKER_INTERACTION_ENERGY, LigScore1, LigScore2, PLP1, PLP2, Jain, PMF, and PMF04) and consensus scoring functions in an attempt to accurately predict the binding affinities between ligand molecules and their protein receptors. CDOCKER_INTERACTION_ENERGY was more successful in retrieving an accurate pose as the top scorer in the CDOCKER docking ensemble than were the other functions. The best-ranked CDOCKER-calculated original ligand conformation in the protein active site had an all heavy atom root-mean-square deviation (RMSD) value of 0.8496 Å compared to the experimentally determined conformation.

Target compound was docked to the protein active site using CDOCKER protocol, with the same parameters as for the validation of the docking protocol.

## Results and Discussion

### Chemistry

The synthetic pathways for the synthesis of the targeted compounds are illustrated in Scheme 1. Starting from 4-aminobenzoic acid (**1**), ethyl 4-amino-3-nitrobenzoate (**5**) was synthesized via acetylation, nitration, hydrolysis and esterification reactions according to previously reported procedures.[22] Acetylation of **5** with chloroformate gave **6a**. Reduction of the nitro group of **6a** gave compound **7a**, which was submitted to reaction with CDI in anhyrdrous THF to afford **8a**. Introduction of isopropyl group in the structure of **8a** was possible via reaction of it with 2-iodo propane. This sequence gave **9a**. Finally, the carboalkoxy group was removed in TFA solution to obtain the intermediate ethyl 1-isopropyl-2-oxo-2,3-dihydro-1*H*-benzo[*d*]imidazole-6-carboxylate (**10a**). Another intermediate, ethyl 1-isopropyl-2-oxo-2,3-dihydro-1*H*-benzo[*d*]-imidazole-5-carboxylate (**8b**) was prepared from **5** via Borch reduction with acetone, reduction with $Na_2S_2O_4$ and cyclization with triphosgene.[23] The title compounds, **11a01**-**11a15** and **9b01**-**9b21** were prepared according to our previous publication.[14-16]

### Antifungal activities

The newly synthesized compounds were evaluated for their antifungal activity against *B. cinerea* by spore germination assay. Most of the tested compounds had inhibitory effect on spore germination, among which **11a03**, **11a04**, **11a06**, **11a08**, **11a10**, **9b10**, **9b19** and **9b21** showed excellent activity (Table 1).

As shown in Table 1, the antifungal activities of **11a11**, **9b11** and **9b20** were lower than that of **11a10**, **9b10** and **9b19**, which implied that introducing substitution at β-position was not beneficial to the activity of α,β-unsaturated acyl derivatives. But this was not justified by the strong activity of **9b21**. Another thing we noted was that the activities of **9b19** and **9b21** were dramatically higher than that of other 5-carboxylate substituted derivatives. This fact revealed that α,β-unsaturated acyl derivatives had different mechanism of action, and it could be attributed to Michael-type addition reaction under physiological conditions.[24]

Comparison between the 5- and 6-carboxylate substituted derivatives revealed that the latter had stronger antifungal activity than the former. It implied that the activity was affected by the substituted position of carboxylate at benzene ring of benzimidazolone, and introducing carboxylate at 6-position was favorable to the activity. **11a03**, **11a04** and **11a14** exhibited stronger antifungal activity than other aliphatic acyl derivatives, and it revealed that the activity requires specific length or size of the alkyl groups. Meanwhile, the difference of activities between **11a01** and **11a06** indicated that the introduction of 4-chloro-phenoxyl at α-position of acetyl increased the fungicidal activity to a large extent. The antifungal activities of all substituted benzoyl derivatives were

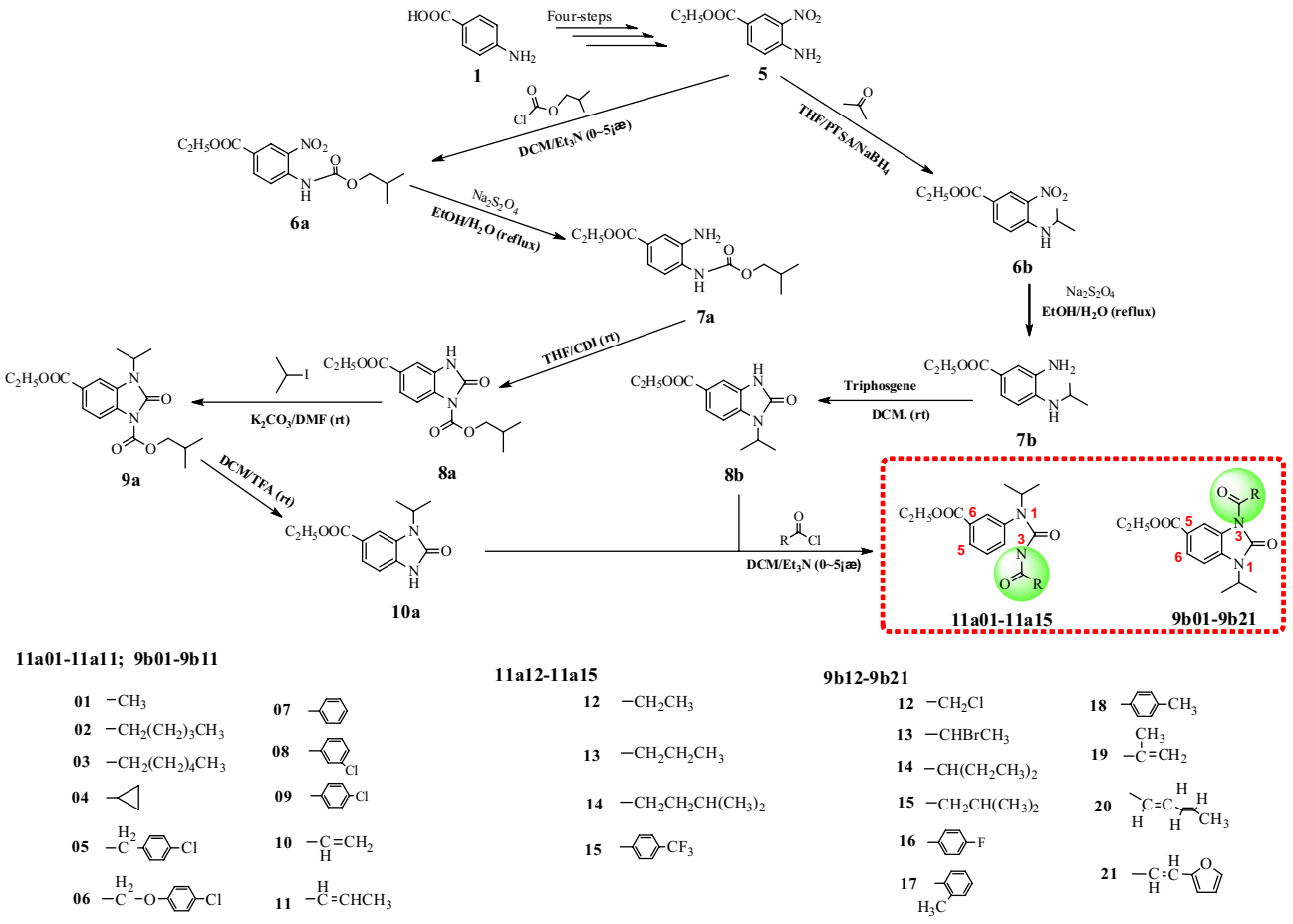


**Scheme 1.** Synthesis of compounds **11a01-11a15** and **9b01-9b21**.

higher than that of **11a07**, and it implied that the activity of benzoyl derivatives could be increased by introducing chlorine and fluorine atoms. In view of the weak activity, the results of 5-carboxylate substituted derivatives were not discussed here.

## QSAR studies

Thirty-six *N*-acylated benzimidazolone carboxylates with antifungal activity were studied in the investigation, and the antifungal activity data were expressed as inhibition percentage and transferred as *D* values. The compounds were randomly split into training and testing sets for QSAR study (28 compounds as training sets and 8 compounds as test sets). Selection of the training and test sets was done by considering the fact that the test compounds represent structural diversity and a range of biological activities similar to that of the training set (Table 1). The min and max activities (*D* values) of the training set compounds were 1.35 and 3.46, respectively, and those in the test set compounds were 1.62 and 3.32, respectively. The semi-empirical AM1 calculation was performed for the conformation search, and various physicochemical properties (96) were selected as descriptors used for QSAR construction from Discovery Studio 4.0. A reliable QSAR model should be validated with some statistical indexes and was validated by the external test set. In order to check the credibility of the models, several parameters were used, such as squared correlation coefficient ($R^2$) and adjusted squared correlation coefficient (Adj-$R^2$). Leave-one-out cross-validation $R^2$ ($Q^2$) was employed to validate the generated QSAR equations.

QSAR model was generated by GFA and PLS statistical analysis according to 36 compounds. However, both the GFA and PLS models showed low $R^2$ values and low predictive powers in an external test set (Table 2). To obtain optimal QSAR model, α,β-unsaturated acyl derivatives were eliminated from the training and test sets. As Michael reaction acceptors, their activity was not solely determined by benzimidazolone scaffold. After excluding α,β-unsaturated acyl derivatives, the min and max activities (*D* values) of the training set compounds were 1.35 and

**Table 1.** Comparison of antifungal activities between experimental data and QSAR prediction, and docking scores

| Compound | Molecular properties | | | Exp. (*D*/Pct.) | GFATempModel_1 | | PLSTempModel_1 | | Docking scores |
|---|---|---|---|---|---|---|---|---|---|
| | Molecular weight | CHI_3_P | Dipole_Y | | Pred. (*D*) | Residual | Pred. (*D*) | Residual | |
| Training set | | | | | | | | | |
| **11a02** | 346.421 | 8.4373 | 0.7622 | 2.83/66.06 | 2.84 | –0.01 | 2.80 | 0.03 | 51.33 |
| **11a03** | 360.447 | 8.6873 | 0.7076 | 2.99/73.09 | 2.96 | 0.03 | 2.88 | 0.11 | 56.03 |
| **11a05** | 400.855 | 10.0148 | 2.4881 | 2.46/41.63 | 2.27 | 0.19 | 2.33 | 0.13 | 53.55 |
| **11a06** | 416.855 | 10.3400 | 0.7018 | 3.03/71.87 | 3.12 | –0.09 | 3.14 | –0.11 | 57.30 |
| **11a07** | 352.384 | 9.5177 | 0.9465 | 2.34/38.49 | 2.48 | –0.14 | 2.50 | –0.16 | 48.93 |
| **11a08** | 386.829 | 9.8449 | 0.72695 | 3.01/72.48 | 2.90 | 0.11 | 3.04 | –0.03 | 52.84 |
| **11a09** | 386.829 | 9.9284 | 1.4111 | 2.82/62.97 | 2.58 | 0.24 | 2.62 | 0.20 | 52.21 |
| **11a10** | 302.325 | 7.8182 | 0.9961 | 3.46/90.59 | – | – | – | – | 47.11 |
| **11a11** | 316.352 | 7.9183 | 0.8217 | 2.20/33.47 | – | – | – | – | 46.83 |
| **11a12** | 304.341 | 7.8182 | 1.0163 | 2.55/53.56 | 2.41 | 0.14 | 2.50 | 0.05 | 46.59 |
| **11a14** | 346.421 | 8.3736 | 1.0343 | 2.90/69.72 | 2.75 | 0.15 | 2.69 | 0.21 | 51.92 |
| **11a15** | 420.382 | 10.8645 | 1.7672 | 2.49/42.26 | 2.54 | –0.05 | 2.52 | –0.03 | 55.87 |
| **9b01** | 290.314 | 7.2870 | 2.7658 | 1.58/11.60 | 1.66 | –0.08 | 1.64 | –0.06 | 49.32 |
| **9b03** | 360.447 | 8.6873 | 2.6828 | 1.97/20.44 | 2.11 | –0.14 | 1.92 | 0.05 | 47.57 |
| **9b04** | 316.352 | 8.2013 | 2.6989 | 1.66/12.71 | 1.71 | –0.05 | 1.71 | –0.05 | 48.89 |
| **9b06** | 416.855 | 10.3400 | 2.4727 | 2.09/22.65 | 2.37 | –0.28 | 2.09 | 0.00 | 47.51 |
| **9b07** | 352.384 | 9.5177 | 2.5653 | 1.75/13.81 | 1.79 | –0.04 | 1.90 | –0.15 | 44.60 |
| **9b08** | 386.829 | 9.8449 | 3.4120 | 2.20/29.28 | 1.75 | 0.45 | 1.89 | 0.31 | 45.66 |
| **9b11** | 316.352 | 7.9183 | 2.6339 | 1.52/9.39 | – | – | – | – | 47.37 |
| **9b12** | 324.759 | 7.8182 | 4.0165 | 1.63/11.61 | 1.38 | 0.25 | 1.28 | 0.35 | 48.14 |
| **9b13** | 383.237 | 8.1759 | 3.5523 | 2.05/22.65 | 2.19 | –0.14 | 2.34 | –0.29 | 46.54 |
| **9b14** | 346.421 | 8.9167 | 2.7456 | 1.35/6.08 | 1.83 | –0.48 | 1.72 | –0.37 | 46.47 |
| **9b15** | 318.368 | 8.1759 | 2.6934 | 1.73/13.81 | 1.75 | –0.02 | 1.76 | –0.03 | 50.11 |
| **9b16** | 370.374 | 9.9284 | 3.3375 | 1.64/10.50 | 1.55 | 0.09 | 1.58 | 0.06 | 44.53 |
| **9b17** | 366.41 | 9.9775 | 2.7964 | 1.58/9.39 | 1.71 | –0.13 | 1.79 | –0.21 | 43.79 |
| **9b19** | 316.352 | 8.1759 | 2.7714 | 3.11/80.26 | – | – | – | – | 50.53 |
| **9b20** | 342.389 | 8.4373 | 2.5023 | 2.08/25.97 | – | – | – | – | 49.19 |
| **9b21** | 368.383 | 9.6793 | 3.9076 | 3.33/85.34 | – | – | – | – | 51.63 |
| Test set | | | | | | | | | |
| **11a01** | 290.314 | 7.2870 | 1.0789 | 2.40/46.65 | 2.47 | –0.07 | 2.49 | –0.09 | 46.59 |
| **11a04** | 316.352 | 8.2012 | 0.9575 | 2.92/72.48 | 2.52 | 0.40 | 2.47 | 0.45 | 50.82 |
| **11a13** | 318.368 | 7.9183 | 1.0267 | 2.29/37.87 | 2.55 | –0.26 | 2.54 | –0.25 | 51.11 |
| **9b02** | 346.421 | 8.4373 | 2.6843 | 1.70/12.71 | 1.92 | –0.22 | 1.88 | –0.18 | 48.27 |
| **9b05** | 400.855 | 10.0148 | 3.9989 | 1.62/9.39 | 1.55 | 0.07 | 1.55 | 0.07 | 42.69 |
| **9b09** | 386.829 | 9.9284 | 3.0444 | 1.79/13.81 | 1.88 | –0.09 | 1.91 | –0.12 | 50.28 |
| **9b10** | 302.325 | 7.8182 | 2.5567 | 3.32/87.32 | – | – | – | – | 47.60 |
| **9b18** | 366.41 | 9.9284 | 2.4939 | 2.20/29.28 | 1.80 | 0.40 | 1.91 | 0.29 | 51.75 |

Molecular weight: the sum of the atomic masses; CHI_3_P: topological connectivity indices, which are a special class of descriptors that do not rely on a three-dimensional model but derived from the two-dimensional topology of the molecule; Dipole_Y: 3D electronic descriptors that indicate the strength and orientation behavior of a molecule in an electrostatic field; Pct.: inhibition percentage. *D* values close to 3 are considered as excellent activity.

3.03, respectively, and those in the test set compounds were 1.62 and 2.92, respectively. Finally, the best-derived QSAR model was presented by the following estimated tri-parametric equation with correlation coefficient ($R^2$) = 0.8719. The most relevant descriptors derived for modeling the antifungal activity were shown in Table 1. The relation between the experimental and predicted values for antifungal activities is illustrated in Figure 1.

$$\text{Antifungal activity } (D \text{ values}) = 1.6024 - 0.42853 \times \text{Dipole\_Y} - 0.329 \times \text{CHI\_3\_P} + 0.012533 \times \text{Molecular weight} \quad (2)$$

As seen in equation 2, the developed QSAR model by GFA statistical analysis indicated that descriptor of molecular weight showed positive correlation with antifungal activity, whereas descriptors of CHI_3_P and

**Table 2.** Summary of GFA and PLS models of benzimidazolones

| Model | $R^2$ | $R^2_{adj}$ | $R^2_{pred}$ | $Q^2_{ext}$ |
|---|---|---|---|---|
| GFA_Model_1 | 0.8719 | 0.8488 | 0.8113 | 0.611 |
| GFA_Model_2 | 0.6810 | 0.6455 | 0.6061 | 0.305 |
| PLS_Model_1 | 0.8955 | 0.8730 | 0.5780 | 0.689 |
| PLS_Model_2 | 0.3590 | 0.3080 | 0.1800 | 0.253 |

Model_1 was generated by 29 compounds (22 in training sets and 7 in test sets); Model_2 was generated by 36 compounds (28 in training sets and 8 in test sets). $R^2$ is the coefficient of determination; $R^2_{adj}$ is $R^2$ adjusted for the number of terms in the model; $R^2_{pred}$ is the prediction (PRESS) $R^2$, equivalent to $Q^2$ from a leave-one-out cross-validation; $Q^2_{ext}$ is the $Q^2$ of models using external test set validation.

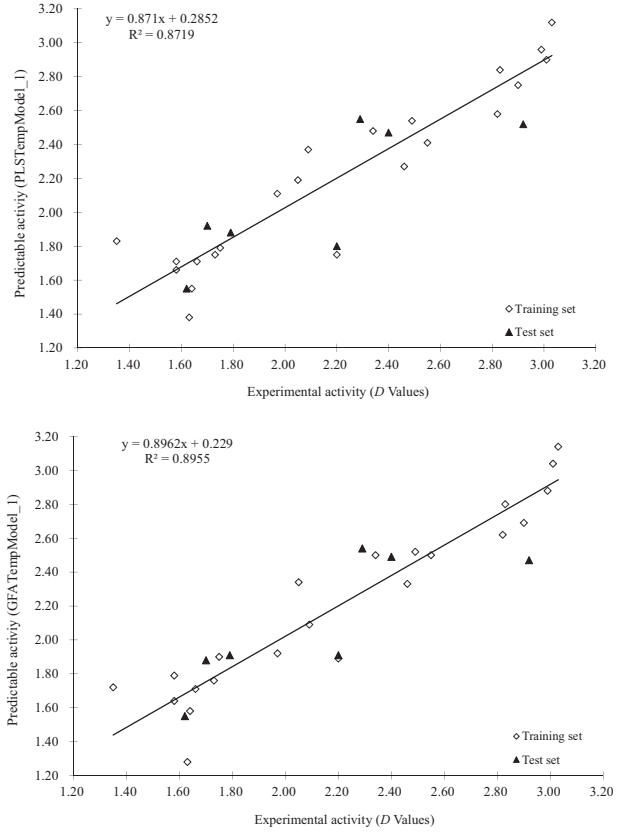


**Figure 1.** Plot of observed *vs*. predicted antifungal activities (*D* values) of benzimidazolones.

Dipole_Y showed negative correlation with antifungal activity.

Molecular weight, Dipole_Y and CHI_3_P were in agreement with the experimental data and were analyzed herein. **11a06** (*D* = 3.03) was the most active compound among aliphatic acyl derivatives of 6-carboxylate substituted benzimidazolone, and it has the molecular weight = 416.86 (positive correlation), Dipole_Y = 0.7018 and CHI_3_P = 10.34 (negative correlation). Its analogue, **11a05** (*D* = 2.46), possesses molecular weight of 400.855, Dipole_Y value of 2.4881 and CHI_3_P value of 10.01. Meanwhile, the positive correlation between activity and descriptors was also observed among benzoyl derivatives. The activities of **11a07** (*D* = 2.34) and **11a15** (*D* = 2.49) were weaker than that of **11a08** (most active compound among benzoyl derivatives, *D* = 3.01), due to the small molecular weight and large value of Dipole_Y, respectively.

Although they only exhibited moderate antifungal activity, 5-carboxylate substituted benzimidazolones showed similar tendency between antifungal activities and molecular weight, Dipole_Y and CHI_3_P.

In addition, variation in antifungal activities of the 5- and 6-substituted regioisomers of benzimidazolone could also be explained by the values of Dipole_Y, since regioisomers have the same molecular weight and CHI_3_P values. It was observed a correlation between antifungal activities of 5- and 6-substituted regioisomers and Dipole_Y values. The compounds with higher biological activity (in this case, the 6-substituted derivatives) presented smaller Dipole-Y values compared to the 5-substituted derivatives.

## Target prediction and molecular docking

Potential targets of the title compounds were predicted *in silico* using default setting of ligand profiling methods from PharmaDB Pharmacophore database and validated by molecular docking based on Discovery Studio 4.0 software.

According to the fit values and function analysis of the obtained proteins, the enoyl acyl carrier protein reductase InhA (fatty acid synthetase) was screened as potential target for the title compounds from scPDB database.[25] The protein structures (2NSD) were downloaded from the Protein Data Bank, and docked with title compounds using CDOCKER protocol for target validation. Validation was done on the target by computing the correlation of the docking scores (CDOCKER_INTERACTION_ENERGY) with antifungal activity (Table 1, Figure 2). As shown in Figure 2,

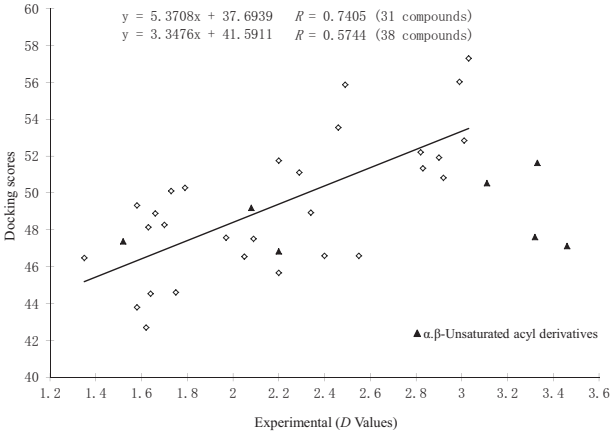


**Figure 2.** Plot of antifungal activities (*D* values) *vs*. docking scores.

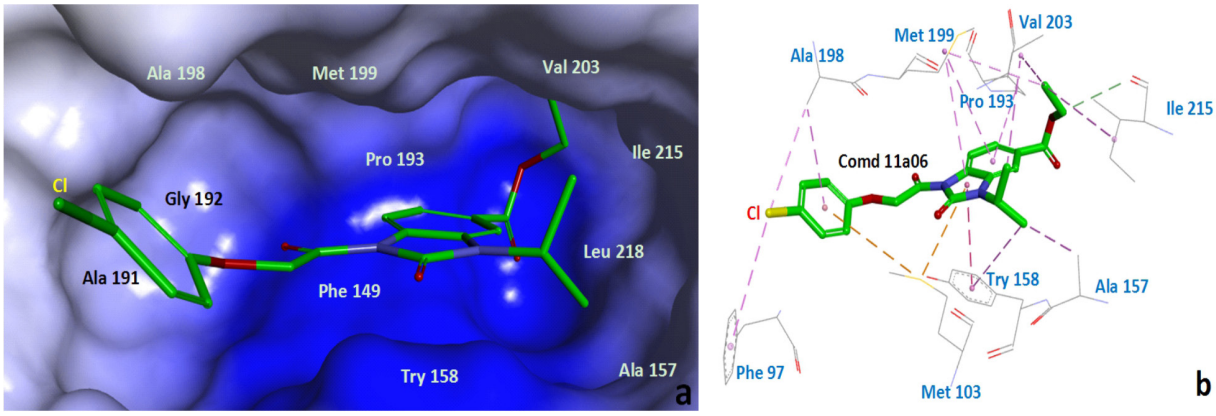


**Figure 3.** Structure of **11a06** bound to the fatty acid synthetase active site by molecular docking (PDB code: 2NSD).

obtained protein with the *R* value of 0.7405 showed a good correlation between docking scores and *D* values.

To understand the interaction mode of title compounds bound to the InhA active site, compound **11a06** as a reference, details of interaction between ligand and obtained protein can be seen in Figure 3. The results indicate that the compound docks well and interacts with important residues of the InhA binding site. The benzimidazolone ring of **11a06** fit nicely into the binding pocket and formed hydrophobic interaction with the hydrophobic residues of Phe97, Met103, Phe149, Ala157, Try158, Pro193, Ala198, Met199, Val203 and Leu218 (π-π stacking interactions, π-alkyl interactions, alkyl interactions and π-sulfur interactions), which is the one primary binding interaction.[26] Compound **11a06** also is observed to form a hydrogen bond interaction with residue Ile215 at the binding pocket. Additionally, it is worthwhile to note that there is still space in the vicinity of Ala191 and Gly192 (Figure 3a). The large cavum suggesting that the introduction of bulky hydrophobic substituents might provide more hydrophobic contacts between the inhibitor and hydrophobic residues, and which will be studied in the future.

To further justify the conclusion, the experiment which was used to screen fatty acid synthesis inhibitors was carried out.[26] The results indicated that the inhibition percentage of **11a03**, **11a04**, **11a06**, **11a08** and **11a14** on the spore germination of *B. cinerea* were 73.09, 72.48, 71.87, 72.48 and 69.72%, and the values were reduced to 22.22, 21.32, 27.00, 16.33 and 17.30% by the addition of the exogenous sodium stearate to spore suspension (Table 3). This phenomenon is consistent with the fact that the activity of fatty acid synthase (FAS)-targeting antimicrobial agents could be mitigated when culture media was supplemented with long-chain fatty acids.[27] Further investigations into the mechanism of action and structural modification of benzimidazolones are continuing in our laboratories.

**Table 3.** The effects of exogenous fatty acids on the antifungal activity of benzimidazolones

| Compound | Mean inhibition / % | |
|---|---|---|
| | Benzimidazolones | Benzimidazolones + sodium stearate |
| **11a03** | 73.09 | 22.22 |
| **11a04** | 72.48 | 21.32 |
| **11a06** | 71.87 | 27.00 |
| **11a08** | 72.48 | 16.33 |
| **11a14** | 69.72 | 17.30 |

## Conclusions

In this study novel *N*-acylated benzimidazolone derivatives were synthesized and their antifungal activities were examined. 6-carboxylate substituted derivatives showed better antifungal activity than its 5-substituted regioisomers. 2D-QSAR studies revealed good predictive and statistically significant QSAR models, as well as highlighted that the activities were strongly influenced by the type of introduced acyl groups in the benzimidazolone moiety.

Potential targets of the title compounds were predicted using ligand profiling and validated by molecular docking, and the results implied that the title compounds might be a new type of fatty acid synthetase inhibitor.

## Supplementary Information

Supplementary information is available free of charge at http://jbcs.sbq.org.br as a PDF file.

## Acknowledgments

This study was supported in part by the grant of the National Natural Science Foundation of China (No.

31371973, 31301700), the Natural Science Foundation of Shaanxi Province (No. 2013JQ3003), and the Fundamental Research Funds for the Central Universities (QN2013009).

## References


1. Monforte, A.-M.; Rao, A.; Logoteta, P.; Ferro, S.; Luca, L. D.; Barreca, M. L.; Iraci, N.; Maga, G.; Clercq, E. D.; Pannecouque, C.; Chimirri, A.; *Bioorg. Med. Chem.* **2008**, *16*, 7429.
2. Theberge, C. R.; Bednar, R. A.; Bell, I. M.; Corcoran, H. A.; Fay, J. F.; Hershey, J. C.; Johnston, V. K.; Kane, S. A.; Mosser, S.; Salvatore, C. A.; Williams, T. M.; Zartman, C. B.; Zhang, X. F.; Graham, S. L.; Vacca, J. P.; *Bioorg. Med. Chem. Lett.* **2008**, *18*, 6122.
3. Wang, W.; Cao, H. P.; Wolf, S.; Camacho-Horvitz, M. S.; Holak, T. A.; Dömling, A.; *Bioorg. Med. Chem.* **2013**, *21*, 3982.
4. Omura, H.; Kawai, M.; Shima, A.; Iwata, Y.; Ito, F.; Masuda, T.; Ohta, A.; Makita, N.; Omoto, K.; Sugimoto, H.; Kikuchi, A.; Iwata, H.; Ando, K.; *Bioorg. Med. Chem. Lett.* **2008**, *18*, 3310.
5. Palin, R.; Bom, A.; Clark, J. K.; Evans, L.; Feilden, H.; Houghton, A. K.; Jones, P. S.; Montgomery, B.; Weston, M. A.; Wishart, G.; *Bioorg. Med. Chem.* **2007**, *15*, 1828.
6. Palin, R.; Clark, J. K.; Evans, L.; Houghton, A. K.; Jones, P. S.; Prosser, A.; Wishart, G.; Yoshiizumi, K.; *Bioorg. Med. Chem.* **2008**, *16*, 2829.
7. Berry, J. F.; Ferraris, D. V.; Duvall, B.; Hin, N.; Rais, R.; Alt, J.; Thomas, A. G.; Rojas, C.; Hashimoto, K.; Slusher, B. S.; Tsukamoto, T.; *ACS Med. Chem. Lett.* **2012**, *3*, 839.
8. Ceccarelli, S. M.; Jaeschke, G.; Buettelmann, B.; Huwyler, J.; Kolczewski, S.; Peters, J. U.; Prinssen, E.; Porter, R.; Spooren, W.; Vieira, E.; *Bioorg. Med. Chem. Lett.* **2007**, *17*, 1302.
9. Sivendran, S.; Jones, V.; Sun, D. Q.; Wang, Y.; Grzegorzewicz, A. E.; Scherman, M. S.; Napper, A. D.; McCammon, J. A.; Lee, R. E.; Diamond, S. L.; McNeil, M.; *Bioorg. Med. Chem.* **2010**, *18*, 896.
10. Bruncko, M.; Tahir, S. K.; Song, X.; Chen, J.; Ding, H.; Huth, J. R.; Jin, S.; Judge, R. A.; Madar, D. J.; Park, C. H.; Park, C. M.; Petros, A. M.; Tse, C.; Rosenberg, S. H.; Elmore, S. W.; *Bioorg. Med. Chem. Lett.* **2010**, *20*, 7503.
11. Liu, W. G.; Lau, F.; Liu, K.; Wood, H. B.; Zhou, G. C.; Chen, Y. L.; Li, Y.; Akiyama, T. E.; Castriota, G.; Einstein, M.; Wang, C. L.; McCann, M. E.; Doebber, T. W.; Wu, M.; Chang, C. H.; McNamara, L.; McKeever, B.; Mosley, R. T.; Berger, J. P.; Meinke, P. T.; *J. Med. Chem.* **2011**, *54*, 8541.
12. Messaoudi, S.; Sancelme, M.; Polard, H. V.; Aboab, B.; Moreau, P.; Prudhomme, M.; *Eur. J. Med. Chem.* **2004**, *39*, 453.
13. Vira, J. J.; Patel, D. R.; Bhimani, N. V.; Ajudia, P. V.; *Pharma Chem*. **2010**, *2*, 178.
14. Li, S. K.; Ji, Z. Q.; Zhang, J. W.; Guo, Z. Y.; Wu, W. J.; *J. Agric. Food Chem.* **2010**, *58*, 2668.
15. Li, F. F.; Wei, S. P.; Zong, Z. F.; Ji, Z. Q.; *Chin. J. Pestic. Sci.* **2012**, *14*, 597.
16. Wei, S. P.; Wu, W. J.; Ji, Z. Q.; *Int. J. Mol. Sci.* **2012**, *13*, 4819.
17. Accelrys Software; *DISCOVERY STUDIO Version* 4.0; San Diego, CA, 2013.
18. Duchowicz, P. R.; Vitale, M. G.; Castro, E. A.; Fernández, M.; Caballero, J.; *Bioorg. Med. Chem.* **2007**, *15*, 2680.
19. Meslamani, J.; Li, J. B.; Sutter, J.; Stevens, A.; Bertrand, H.-O.; Rognan, D.; *J. Chem. Inf. Model.* **2012**, *52*, 943.
20. http://bioinfo-pharma.u-strasbg.fr/scPDB accessed in December 2014.
21. http://www.rcsb.org/pdb/explore/explore.do?structureId=2nsd accessed in December 2014.
22. Zhang, Y. M.; White, S. W.; Rock, C. O.; *J. Biol. Chem.* **2006**, *281*, 17541.
23. McClure, K. F.; Abramov, Y. A.; Laird, E. R.; Barberia, J. T.; Cai, W. L.; Carty, T. J.; Cortina, S. R.; Danley, D. E.; Dipesa, A. J.; Donahue, K. M.; *J. Med. Chem.* **2005**, *48*, 5728.
24. Stack, V. T.; *Ind. Eng. Chem.* **1957**, *49*, 913.
25. He, X.; Alianc, A.; Montellano, P. R. O.; *Bioorg. Med. Chem.* **2007**, *15*, 6649.
26. Prosen, K. R.; Carroll, R. K.; Burda, W. N.; Krute, C. N.; Bhattacharya, B.; Dao, M. L.; Turos, E.; Shaw, L. N.; *Bioorg. Med. Chem. Lett.* **2011**, *20*, 5293.
27. Brinster, S.; Lamberet, G.; Staels, B.; Trieu-Cuot, P.; Gruss, A.; Poyart, C.; *Nature* **2009**, *458*, 83.


*Submitted: August 24, 2014*
*Published online: February 6, 2015*